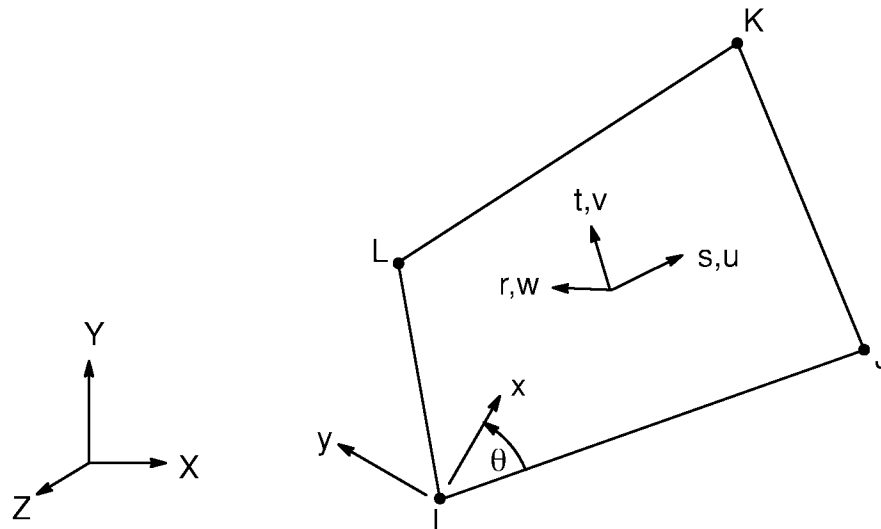


# 14.43 SHELL43 — Plastic Shell



Matrix or Vector	Geometry	Shape Functions	Integration Points
Stiffness Matrix	Quad	Equations (12.5.13-1), (12.5.13-2), and (12.5.13-3)	In-plane: 2 x 2 Thru-the-thickness: 2 (linear material) 5 (nonlinear material)
	Triangle	Equations (12.5.4-1), (12.5.4-2), and (12.5.4-3)	In-plane: 1 Thru-the-thickness: 2 (linear material) 5 (nonlinear material)
Mass Matrix	Quad	Equations (12.5.8-1), (12.5.8-2), and (12.5.8-3)	Same as stiffness matrix
	Triangle	Equations (12.5.1-1), (12.5.1-2), and (12.5.1-3)	Same as stiffness matrix
Stress Stiffness Matrix	Same as mass matrix		Same as stiffness matrix

Matrix or Vector	Geometry	Shape Functions	Integration Points
Thermal Load Matrix	Same as stiffness matrix		Same as stiffness matrix
Transverse Pressure Load Vector	Quad	Equation (12.5.8–3)	2 x 2
	Triangle	Equation (12.5.1–3)	1
Edge Pressure Load Vector	Quad	Equations (12.5.8–1) and (12.5.8–2) specialized to the edge	2
	Triangle	Equations (12.5.1–1) and (12.5.1–2) specialized to the edge	2

Load Type	Distribution
Element Temperature	Bilinear in plane of element, linear thru thickness
Nodal Temperature	Bilinear in plane of element, constant thru thickness
Pressure	Bilinear in plane of element and linear along each edge

References: Ahmad(1), Cook(5), Dvorkin(96), Dvorkin(97), Bathe and Dvorkin(98), Allman(113), Cook(114), MacNeal and Harder(115)

### 14.43.1 Other Applicable Sections

Chapter 2 describes the derivation of structural element matrices and load vectors as well as stress evaluations. Section 13.1 describes integration point locations.

### 14.43.2 Assumptions and Restrictions

Normals to the centerplane are assumed to remain straight after deformation, but not necessarily normal to the centerplane.

Each pair of integration points (in the r direction) is assumed to have the same element (material) orientation.

This element does not generate a consistent mass matrix; only the lumped mass matrix is available.

### 14.43.3 Assumed Displacement Shape Functions

The assumed displacement and transverse shear strain shape functions are given in Chapter 12. The basic shape functions are essentially a condensation of those used for SHELL93. The basic functions for the transverse shear strain have been changed to avoid shear locking (Dvorkin(96), Dvorkin(97), Bathe and Dvorkin(98)) and are pictured in Figure 14.43–1. One result of the use of these displacement and strain shapes is that elastic rectangular elements give constant curvature results for flat elements, and also, in the absence of membrane loads, for curved elements. Thus, for these cases, nodal stresses are the same as centroidal stresses. Both SHELL63 and SHELL93 can have linearly varying curvatures.

### 14.43.4 Stress–Strain Relationships

The material property matrix [D] for the element is:

$$[D] = \begin{bmatrix} AE_x & Av_{xy}E_x & 0 & 0 & 0 & 0 \\ Av_{xy}E_x & AE_y & 0 & 0 & 0 & 0 \\ 0 & 0 & 0 & 0 & 0 & 0 \\ 0 & 0 & 0 & G_{xy} & 0 & 0 \\ 0 & 0 & 0 & 0 & \frac{G_{yz}}{1.2} & 0 \\ 0 & 0 & 0 & 0 & 0 & \frac{G_{xz}}{1.2} \end{bmatrix} \quad (14.43-1)$$

- where:
- $A = \frac{E_y}{E_y - (v_{xy})^2 E_x}$
  - $E_x =$  Young's modulus in element x-direction (input as EX on **MP** command)
  - $v_{xy} =$  Poisson's ratio in element x–y plane (input as NUXY on **MP** command)
  - $G_{xy} =$  shear modulus in element x–y plane (input as GXY on **MP** command)
  - $G_{yz} =$  shear modulus in element y–z plane (input as GYZ on **MP** command)
  - $G_{xz} =$  shear modulus in element x–z plane (input as GXZ on **MP** command)

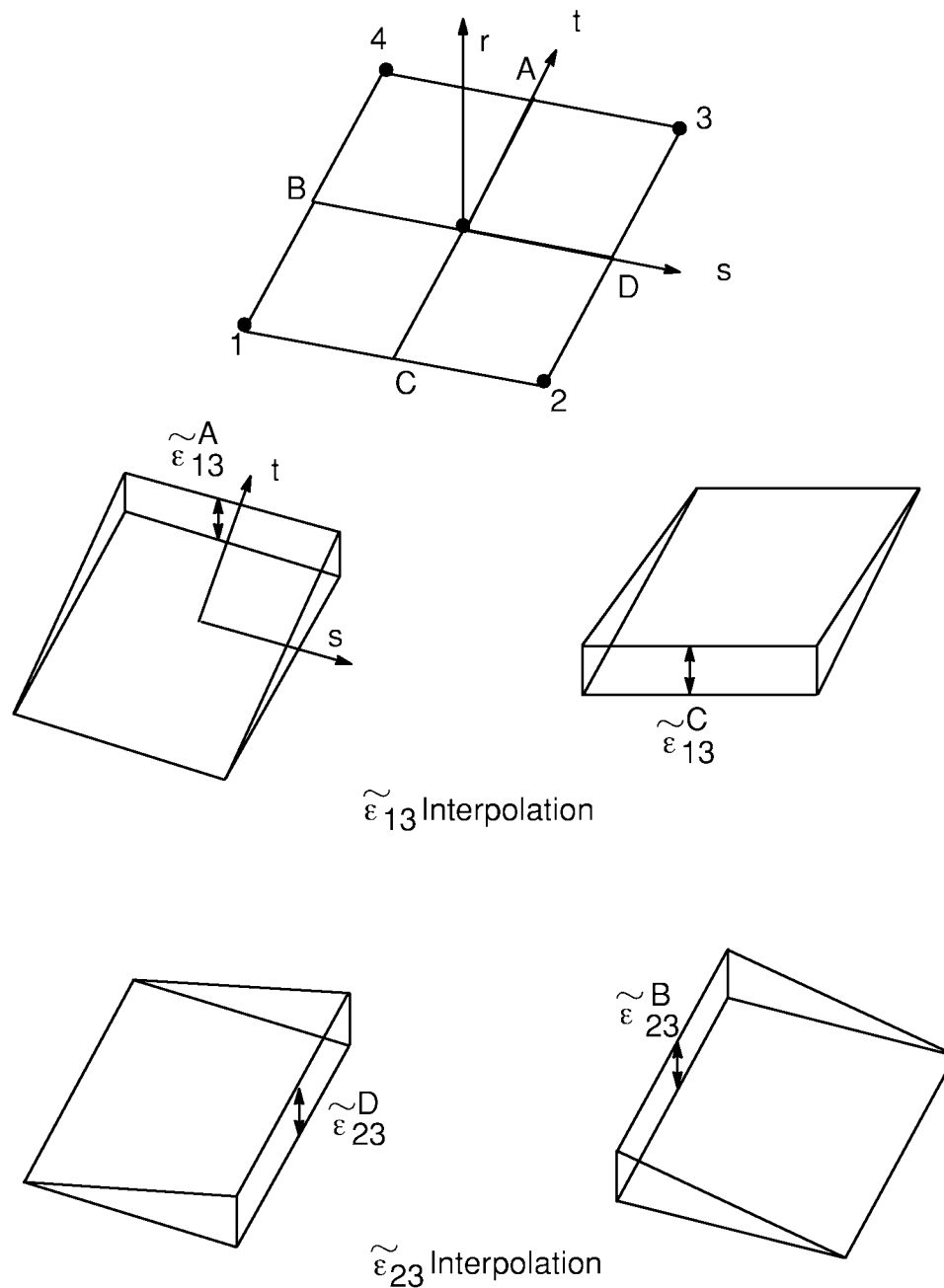


Figure 14.43-1 Shape Functions for the Transverse Strains

### 14.43.5 In-Plane Rotational DOF

If KEYOPT(3) is 0 or 1, there is no significant stiffness associated with the in-plane rotation DOF (rotation about the element  $r$  axis). A nominal value of stiffness is present (as described with SHELL63), however, to prevent free rotation at the node. KEYOPT(3) = 2 is used to include the Allman-type rotational DOFs (as described by

Allman(113) and Cook(114)). Such rotations improve the in-plane and general 3-D shell performance of the element. However, one of the outcomes of using the Allman rotation is that the element stiffness matrix contains up to two spurious zero energy modes (discussed below).

### 14.43.6 Spurious Mode Control with Allman Rotation

The first spurious mode is associated with constant rotations (Figure 14.43–2). The second spurious mode coincides with the well-known hourglass mode induced by reduced order integration (Figure 14.43–3). It is interesting to note that the hourglass spurious mode is elastically restrained for nonrectangular and multi-element configurations.

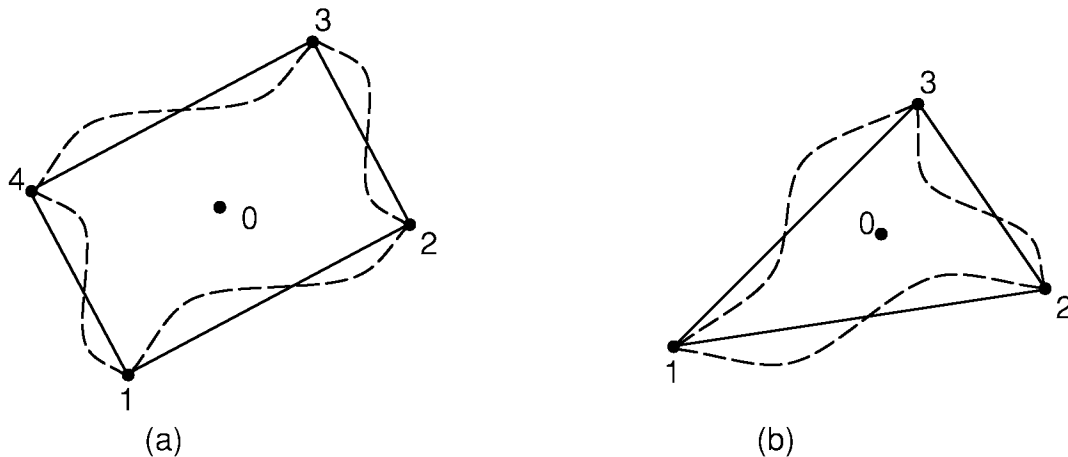


**Figure 14.43–2 Constant in-plane rotation spurious mode**  
 $(\theta_{z1} = \theta_{z2} = \theta_{z3} = \theta_{z4})$

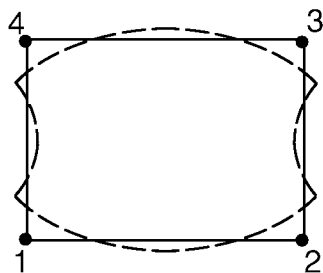


**Figure 14.43–3 Hourglass mode**  $(\theta_{z1} = -\theta_{z2} = \theta_{z3} = -\theta_{z4})$

The spurious modes are controlled on an elemental level using the concept suggested by MacNeal and Harder(115). For the constant rotation (Figure 14.43–2) spurious mode control, an energy penalty is defined as:

$$P_I = \delta_1 V \theta_I G_{xy} \theta_I \quad (14.43-2)$$

where:

- $P_I$  = energy penalty I
- $\delta_1$  = penalty parameter (input quantity ZSTIF1 on **R** command)
- $V$  = element volume
- $G_{xy}$  = shear modulus (input on **MP** command)
- $\theta_I$  = relative rotation, defined below

The relative rotation is computed at the element center as,

$$\theta_I = \theta_o - \frac{1}{n} \sum_{i=1}^n \theta_{zi} \quad (14.43-3)$$

where:

- $\theta_o = \frac{1}{2} \left( \frac{\partial v}{\partial x} \Big|_o - \frac{\partial u}{\partial y} \Big|_o \right)$
- $u, v$  = in-plane motions assuming edges remain straight
- $\theta_{zi}$  = in-plane rotation at node i
- $n$  = number of nodes per element
- $\Big|_o$  = evaluated at center of element

For the hourglass spurious modes which occur only for 4-noded elements, the energy penalty is taken as the inner product of the constraint force vector and the alternating rotational mode shapes as,

$$P_{II} = \delta_2 V \theta_{II} G_{xy} \theta_{II} \quad (14.43-4)$$

where:

- $P_{II}$  = energy penalty II
- $\delta_2$  = penalty parameter (input quantity ZSTIF2 on **RMORE** command)
- $\theta_{II} = \frac{1}{4} (\theta_{z1} - \theta_{z2} + \theta_{z3} - \theta_{z4})$

Once the energy penalties ( $P_I$  and  $P_{II}$ ) are defined, the associated stiffness augmentations can be calculated as,

$$\left[ K_{ij}^e \right]_a = \frac{\partial^2 P_I}{\partial u_i \partial u_j} + \frac{\partial^2 P_{II}}{\partial u_i \partial u_j} \quad (14.43-5)$$

where:  $u_i$  = nodal displacement vector

This augmented stiffness matrix when added to the regular element stiffness matrix results in an effective stiffness matrix with no spurious modes.

### 14.43.7 Natural Space Extra Shape Functions with Allman Rotation

One of the outcomes of the Allman rotation is the dissimilar displacement variation along the normal and tangential directions of the element edges. The result of such variation is that the in-plane bending stiffness of the elements is too large by a factor  $1/(1-\nu^2)$  and sometimes termed as Poisson's ratio locking. To overcome this difficulty, two natural space (s and t) nodeless in-plane displacement shape functions are added in the element stiffness matrix formulation and then condensed out at the element level. The element thus generated is free of Poisson's ratio locking. For details of a similar implementation, refer to Yunus et al (117).

### 14.43.8 Warping

A warping factor is computed as:

$$\phi = \frac{D}{t} \quad (14.43-6)$$

where:

- D = component of the vector from the first node to the fourth node parallel to the element normal
- t = average thickness of the element

If  $\phi > 1.0$ , a warning message is printed.

### 14.43.9 Stress Output

The stresses at the center of the element are computed by taking the average of the four integration points on that plane.

The output forces and moments are computed as described in Section 2.3.